

Adaptive Fuzzy C-Means with Graph Embedding

Qiang Chen, Weizhong Yu, Feiping Nie, and Xuelong Li

Abstract—Fuzzy clustering algorithms can be roughly categorized into two main groups: Fuzzy C-Means (FCM) based methods and mixture model based methods. However, for almost all existing FCM based methods, how to automatically selecting proper membership degree hyper-parameter values remains a challenging and unsolved problem. Mixture model based methods, while circumventing the difficulty of manually adjusting membership degree hyper-parameters inherent in FCM based methods, often have a preference for specific distributions, such as the Gaussian distribution. In this paper, we propose a novel FCM based clustering model that is capable of automatically learning an appropriate membership degree hyper-parameter value and handling data with non-Gaussian clusters. Moreover, by removing the graph embedding regularization, the proposed FCM model can degenerate into the simplified generalized Gaussian mixture model. Therefore, the proposed FCM model can be also seen as the generalized Gaussian mixture model with graph embedding. Extensive experiments are conducted on both synthetic and real-world datasets to demonstrate the effectiveness of the proposed model.

Index Terms—Fuzzy clustering, spectral clustering, fuzzy C-means, Gaussian mixture model, graph embedding.

I. INTRODUCTION

Fuzzy clustering algorithms have been extensively utilized to uncover potential latent structures within data. Typically, fuzzy clustering algorithms can be roughly divided into two main categories: FCM based methods and mixture model based methods.

FCM stands as one of the most classic fuzzy clustering models, forming the cornerstone for numerous existing fuzzy clustering algorithms. The fundamental concept behind FCM is to regulate the fuzziness of membership degrees through hyper-parameters such as weighting exponent [1], [2], entropy regularization [3], or quadratic term [4] hyper-parameters. Although various FCM variants have been developed [5], [6], the challenge still persists in finding a reliable method for

automatically selecting the optimal values of these membership degree hyper-parameters. In almost all existing FCM based clustering algorithms, the membership degree hyper-parameters are adjusted through historical experience or experimental methods. Unfortunately, these approaches are often inefficient and may lead to poor clustering results.

Another drawback of FCM is that it can only achieve good performance on data with spherical clusters, whereas real-world cluster shapes are often complex and non-spherical, such as ellipsoidal and non-Gaussian. To improve the performance of FCM on data with ellipsoidal clusters, Mahalanobis distance was introduced into FCM [7], [8]. For non-Gaussian clusters, some kernel-based FCM algorithms have been developed [9]–[11]. These algorithms can project data from the low-dimensional space to a high-dimensional space, facilitating linear classification of non-Gaussian clusters. However, kernel-based methods are susceptible to noises, and selecting a proper kernel is also a challenging problem.

Recently, graph embedding has become a frequently used technique in machine learning fields because it can help algorithms handle non-Gaussian data [12]–[15]. Spectral clustering is a classic graph based clustering algorithm. It involves constructing graphs to represent samples using an affinity matrix, followed by the application of the K-means algorithm to these graph representations of the data [16]–[18]. Compared to kernel embedding methods, graph embedding methods can better capture the local structure of data and may yield more satisfactory results. Inspired by spectral clustering, lots of graph based clustering algorithms were developed. In order to obtain the optimal graph similarity matrix, Nie et al. proposed a novel model that can automatically learn proper weights of the similarity matrix [19]. To generate a graph with clusters, Han et al. proposed a spectral clustering model that incorporates orthogonal and nonnegative constraints [20]. Moreover, their approach enables the direct acquisition of final cluster labels, eliminating the necessity for post-processing. Pei et al. revisited the unified framework of K-means and ratio-cut spectral clustering, and proposed an efficient clustering algorithm based on the framework [21]. Recently, a novel clustering algorithm utilizing bipartite graphs was also developed [22], which poses an excellent clustering performance but comparatively low computational complexity.

Owing to the excellent performance of graph based methods on non-Gaussian data, various graph based fuzzy clustering algorithms have recently been developed as well. Locality preservation [23] is a proficient graph based dimensional reduction method, and Zhou et al. introduced this method into FCM to enhance clustering performance [24]. To better handle data with balanced clusters, Liu et al. proposed a balance regularization to suppress unbalanced classes. Recently anchor graph is getting a lot of attention, and some anchor graph based

Feiping Nie is the corresponding author.

Qiang Chen is with the School of Computer Science, and School of Artificial Intelligence, Optics and Electronics (iOPEN), Northwestern Polytechnical University, Xi'an 710072, Shaanxi, P. R. China. (e-mail: chengq@mail.nwpu.edu.cn).

Feiping Nie is with the School of Artificial Intelligence, OPTics and ElectroNics (iOPEN), School of Computer Science, Northwestern Polytechnical University, Xi'an 710072, P.R. China, and also with the Key Laboratory of Intelligent Interaction and Applications (Northwestern Polytechnical University), Ministry of Industry and Information Technology, Xi'an 710072, P.R. China (email: feipingnie@gmail.com).

Weizhong Yu is with the School of Artificial Intelligence, OPTics and ElectroNics (iOPEN), Northwestern Polytechnical University, Xi'an 710072, P.R. China, and also with the Key Laboratory of Intelligent Interaction and Applications (Northwestern Polytechnical University), Ministry of Industry and Information Technology, Xi'an 710072, P.R. China (email: yuwz05@mail.xjtu.edu.cn).

Xuelong Li is with the Institute of Artificial Intelligence (TeleAI), China Telecom Corp Ltd, 31 Jinrong Street, Beijing 100033, P. R. China (email: li@nwpu.edu.cn).

clustering methods have been developed [25], [26]. Wang et al. proposed to constraint the sparseness of membership degree matrix utilizing L_0 -norm [27], which may suppress the influence of outliers on graph weights learning and improve clustering performance. Besides, Zhao et al. proposed a novel FCM model featured on shrunk pattern based manifold learning [28], which can be also seen as a graph based method with the same graph weights.

Mixture model based methods can be viewed as the other branch of fuzzy clustering. A mixture model can be seen as a linear combination of multiple probability distributions and is usually optimized by the EM algorithm [29]. The Gaussian mixture model is one of the most popular model based methods [30]. However, the Gaussian mixture model assumes that data is drawn from the Euclidean space. In reality, naturally occurring data may reside on or close to an underlying sub-manifold. For considering the sub-manifold structure, Laplacian regularized Gaussian mixture model and locally consistent Gaussian mixture model were developed [31], [32]. Generally, heavy-tailed distributions are more robust than the Gaussian distribution, such as the generalized Gaussian distribution [33] and the Student's t -distribution [34]. Therefore, some heavy-tailed distributions based mixture models were proposed to improve clustering performance on polluted datasets [35], [36].

By summarizing the above analysis we realize that, for almost all FCM based clustering methods, the problem of automatically learning membership degree hyper-parameters is still challenging and not well-resolved. Additionally, most mixture model based methods only focus on data with specific distributions, i.e., Gaussian distribution, and lack the ability of handling non-Gaussian data. The main contributions of this paper are summarized as follows:

- The proposed FCM model introduces a membership hyper-parameter adaptive learning mechanism that can automatically learn a proper value for the membership degree hyper-parameter.
- By introducing the graph embedding regularization term, the proposed FCM model can handle data with non-Gaussian clusters, which also proves the transferability of the membership hyper-parameter adaptive learning mechanism.
- By removing the graph embedding regularization, the proposed FCM model can degenerate into a simplified generalized Gaussian mixture model. Therefore, the proposed FCM model can be also viewed as a mixture model with graph embedding.
- An efficient alternating optimization strategy with closed solutions is provided to optimize the proposed FCM model.

Notations: Throughout the paper, let \mathbb{R} , \mathbb{R}^+ , \mathbb{R}^n and $\mathbb{R}^{n \times m}$ denote the sets of real numbers, positive real numbers, length- n vectors and size $n \times m$ matrices, respectively. Suppose data matrix $X = [x_1, x_2, \dots, x_n] \in \mathbb{R}^{d \times n}$ consists of n samples with c clusters, and each sample x_i has d features. For matrix A , the element in the i -th row and the j -th column of A is denoted by a_{ij} , and trace of A is denoted by $Tr(A)$. The

adjacency matrix of an undirected weighted graph is defined as W and the degree matrix is defined as D . Then the Laplacian matrix is defined as $L = D - W$, and the normalized one is defined as $\hat{L} = D^{-1/2} L D^{-1/2}$. The L_2 -norm of vector v is denoted by $\|v\|_2$. An identity matrix with n diagonal elements is denoted by I_n .

II. RELATED WORKS

In this section, we introduce some important related works, including FCM, spectral clustering and the generalized Gaussian mixture model.

A. FCM

FCM is an extremely significant fuzzy clustering model as it forms the basis for plenty of fuzzy clustering algorithms. According to the methods of controlling fuzziness, FCM can be roughly divided into three types: weighting exponent based, entropy regularization based, and quadratic term based. The objective function of FCM with entropy regularization is shown below.

$$\begin{aligned} \min_{U, V} \sum_{i=1}^n \sum_{j=1}^c u_{ij} \|x_i - v_j\|_2^2 + \frac{1}{\gamma} u_{ij} \log u_{ij}, \\ \text{s.t. } \sum_{j=1}^c u_{ij} = 1, \quad 0 < u_{ij} < 1 \end{aligned} \quad (1)$$

where $U \in \mathbb{R}^{n \times c}$ denotes the membership degree matrix, $V = \{v_1, v_2, \dots, v_c\}$ denotes the set of cluster centers, $\gamma \in \mathbb{R}^+$ denotes the entropy regularization hyper-parameter, and n and c denote the numbers of samples and clusters, respectively.

Remark 1: In almost all existing FCM with entropy regularization algorithms, the entropy regularization hyper-parameter γ can not be automatically updated. Typically, the value of γ is adjusted by historical experience or experimental results.

B. Spectral Clustering

Spectral clustering is a popular clustering algorithm for its effectiveness on handling non-Gaussian clusters. The fundamental concept behind spectral clustering is the similarity graph that encapsulates pairwise similarities among data points, with higher similarity weights indicating closer proximity. By strategically eliminating weaker edges, the algorithm extracts c independent sub-graphs, ultimately yielding c clusters. However, the optimization of spectral clustering is NP-hard, and it usually resorts to optimizing the following relaxed problems.

$$\min_F Tr(F^T L F), \quad \text{s.t. } F^T F = I_c \quad (2)$$

where $F \in \mathbb{R}^{n \times c}$ is the indicator matrix with c clusters and $L \in \mathbb{R}^{n \times n}$ is the Laplacian matrix. The objective function in Eq. (2) can be optimized by computing the corresponding eigenvectors of the c minimum eigenvalues. Subsequently, performing K-means on F allows us to obtain c clusters. According to the property of Laplacian matrix, the objective function in Eq. (2) can be reformulated as

$$\min_F \frac{1}{2} \sum_{i=1}^n \sum_{j=1}^n w_{ij} \|f_i - f_j\|_2^2 \quad \text{s.t. } F^T F = I_c \quad (3)$$

where w_{ij} is the element of the adjacency matrix W representing the similarity between sample x_i and sample x_j , and $f_i \in \mathbb{R}^{1 \times c}$ is the i -th row of the F . Therefore, the objective function in Eq. (3) can also be seen as a manifold learning algorithm, which projects sample x_i from the original manifold as f_i into the new manifold while preserving the similarities among samples. If the Laplacian matrix L is replaced with the normalized Laplacian matrix \hat{L} , the objective function of R-cut spectral clustering in Eq. (2) is transformed into that of N-cut spectral clustering.

C. Generalized Gaussian Mixture Model

The Kotz-type distribution is a member of the elliptically contoured distribution family, and the generalized Gaussian distribution is a special case of the Kotz-type distribution [37]–[39]. Let $x \in \mathbb{R}^d$ be a d -dimensional random vector, and the probability density function of the generalized Gaussian distribution is defined as follows.

$$g(x|\theta) = \frac{\beta \Gamma(\frac{d}{2}) m^{\frac{d}{2\beta}}}{\pi^{\frac{d}{2}} \Gamma(\frac{d}{2\beta})} |\Sigma|^{-\frac{1}{2}} \times \exp\left\{-m \left[(x-v)^T \Sigma^{-1} (x-v)\right]^\beta\right\} \quad (4)$$

where $\theta = \{v, \Sigma, \beta, m\}$ denotes the set of parameters, $v \in \mathbb{R}^d$ denotes the mean, $\Sigma \in \mathbb{R}^{d \times d}$ denotes the positive definite covariance matrix, $\beta \in \mathbb{R}^+$ denotes the shape parameter, and $m \in \mathbb{R}^+$ denotes the scale parameter.

The generalized Gaussian mixture model can be seen as a linear combination of multiple generalized Gaussian components, and the probability distribution function can be written as

$$f(x|\Theta) = \sum_{j=1}^c \alpha_j g(x|\theta_j), \quad \text{s.t.} \sum_{j=1}^c \alpha_j = 1 \quad (5)$$

where $\Theta = \{\alpha, V, \Sigma, \beta, m\}$ denotes the set of all parameters in the MGGD mixture model, $\theta_j = \{v_j, \Sigma_j, \beta, m\}$ denotes the parameter set of the j -th component, $\alpha = \{\alpha_1, \alpha_2, \dots, \alpha_c\}$ denotes the set of mixing coefficients, and c denotes the number of components.

For estimating the parameters of a probability distribution, the maximum likelihood estimation method is frequently used, and the log-likelihood function is constructed as follows.

$$L(\Theta|X) = \sum_{i=1}^n \log f(x_i|\Theta) = \sum_{i=1}^n \log \sum_{j=1}^c \alpha_j g(x_i|\theta_j), \quad (6)$$

$$\text{s.t.} \sum_{j=1}^c \alpha_j = 1$$

However, optimizing the above objective function presents challenges due to the presence of sum in the logarithm. The Expectation-Maximization (EM) algorithm [40], a probability-based optimization method, is a frequently used method to address this difficulty. Instead of directly optimizing the original objective function, EM introduces a latent variable. The optimization process then shifts towards maximizing the Q function, a derived auxiliary function.

III. THE PROPOSED METHOD

A. Formulation

In this subsection, we initially introduce how the equivalent connection between FCM and the generalized Gaussian mixture model is constructed. Then, based on this, we show how the problem of automatically learning membership degree hyper-parameters in FCM is solved. Furthermore, we introduce how the graph is embedded into FCM to help deal with non-Gaussian clusters, and finally present the objective function of the proposed model.

Equivalence and hyper-parameter learning: Since the log-likelihood function of the generalized Gaussian mixture model involves a sum inside the logarithm, optimizing this objective function requires using the EM algorithm. Notably, the EM algorithm, being grounded in probability theory, diverges significantly from the optimization strategy employed in FCM. In order to build the connection between FCM and the generalized Gaussian mixture model, the equivalent objective function of the generalized Gaussian mixture model is constructed as follows.

Proposition 1: The update equations of the maximum log-likelihood function in Eq. (6) for the generalized Gaussian mixture model, which is optimized through the EM algorithm, are equivalent to the update equations of the following objective function.

$$\min_{U, \alpha, V, \Sigma, \beta, m} \sum_{i=1}^n \sum_{j=1}^c u_{ij} \left\{ m \left[(x_i - v_j)^T \Sigma_j^{-1} (x_i - v_j) \right]^\beta + \frac{1}{2} \log |\Sigma_j| - \log \alpha_j - \log \frac{\beta \Gamma(\frac{d}{2}) m^{\frac{d}{2\beta}}}{\pi^{\frac{d}{2}} \Gamma(\frac{d}{2\beta})} + \log u_{ij} \right\}, \quad (7)$$

$$\text{s.t.} \sum_{j=1}^c \alpha_j = 1, \quad 0 < \alpha_j < 1,$$

$$\sum_{j=1}^c u_{ij} = 1, \quad 0 < u_{ij} < 1$$

where u_{ij} is the membership degree denoting the probability of sample x_i being assigned to the j -th cluster, $\alpha = \{\alpha_1, \alpha_2, \dots, \alpha_c\}$, $V = \{v_1, v_2, \dots, v_c\}$ and $\Sigma = \{\Sigma_1, \Sigma_2, \dots, \Sigma_c\}$ denote the sets of mixing coefficients, means and scale matrices, and β and m denote the shape parameter and the scale parameter in the generalized Gaussian mixture model. To concentrate on the main idea, **the proof for Proposition 1 is moved to the Appendix.**

If we consider only the membership degree matrix U and the set of means V as variables in Eq. (7), treating other variables as constants, i.e., $\Sigma_j = I_d$, $\alpha_j = 1/c$, $\beta = 1$ and $m \in \mathbb{R}^+$, we obtain the objective function of the simplified generalized Gaussian mixture model as follows.

$$\min_{U, V} \sum_{i=1}^n \sum_{j=1}^c u_{ij} m \|x_i - v_j\|_2^2 + u_{ij} \log u_{ij}, \quad (8)$$

$$\text{s.t.} \sum_{j=1}^c u_{ij} = 1, \quad 0 < u_{ij} < 1$$

Then let us look back at the objective function of FCM in Eq. (1). Since the membership degree hyper-parameter γ in FCM

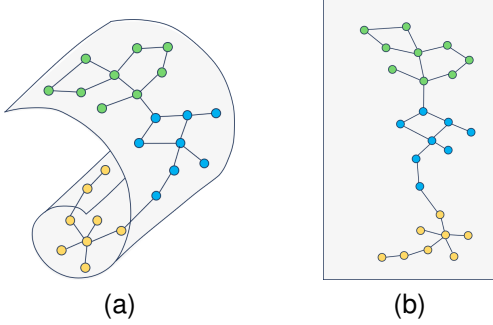


Fig. 1. Illustration on graph based manifold learning. For data residing in a complex manifold, as depicted in (a), Euclidean distance may not accurately capture the true relationships between samples. However, by projecting the data according to the similarity graph into a simpler manifold, as illustrated in (b), the newly learned manifold facilitates easier clustering compared to the original manifold.

is a positive constant, the objective function of FCM in Eq. (1) can be transformed by multiplying γ as follows.

$$\begin{aligned} \min_{U, V} \sum_{i=1}^n \sum_{j=1}^c u_{ij} \gamma \|x_i - v_j\|_2^2 + u_{ij} \log u_{ij}, \\ \text{s.t.} \quad \sum_{j=1}^c u_{ij} = 1, \quad 0 < u_{ij} < 1 \end{aligned} \quad (9)$$

By comparing the objective function of the simplified generalized Gaussian mixture model in Eq. (8) with that of FCM in Eq. (9), we can observe that the membership degree hyper-parameter γ in FCM serves the same purpose as the scale parameter m in the generalized Gaussian mixture model. However, the scale parameter m in the generalized Gaussian model can be learned automatically. Therefore, it is possible to learn the membership degree hyper-parameter γ in FCM in the same manner.

In Eq. (7), if we replace m with γ , consider U, V and γ as variables, and set $\Sigma_j = I_d$, $\alpha_j = 1/c$ and $\beta = 1$, we obtain an FCM objective function that can automatically learn the membership degree hyper-parameter γ as follows.

$$\begin{aligned} \min_{U, V, \gamma} \sum_{i=1}^n \sum_{j=1}^c u_{ij} \gamma \|x_i - v_j\|_2^2 + u_{ij} \log u_{ij} - n \log \gamma^{\frac{d}{2}}, \\ \text{s.t.} \quad \sum_{j=1}^c u_{ij} = 1, \quad 0 < u_{ij} < 1 \end{aligned} \quad (10)$$

where d is the number of features for sample x_i . Note that, the FCM objective function in Eq. (10) can be also seen as a simplified generalized Gaussian mixture model, because they have the same update equations.

Graph embedding and the proposed model: A drawback of FCM is that it may not perform well with non-spherical clusters because it relies directly on Euclidean distance. However, real-world data are often non-spherical and non-Gaussian. A frequently used method for handling non-Gaussian data is graph based manifold learning. It constructs a similarity graph of the data and then projects them according to these similarities from the original manifold into a new manifold where the data can be more effectively clustered.

An illustration of graph based manifold learning is shown in Fig. 1.

A key point for graph based manifold learning is graph construction. Membership degree u_{ij} in FCM denotes the probability of the i -th sample belonging to the j -th cluster, but it can also be used to reveal the latent relationships between samples. Therefore, it is possible to construct a new similarity graph, based on the membership degrees, to help complete the original similarity graph. If the update equation of cluster center v_j can be represented as $v_j = \sum_{i=1}^n u_{ij} x_i / \sum_{i=1}^n u_{ij}$, we have the following equation.

$$\sum_{i=1}^n \sum_{j=1}^c u_{ij} \|x_i - v_j\|_2^2 = \text{Tr} [X(I_n - UBU^T)X^T] \quad (11)$$

where $X = [x_1, x_2, \dots, x_n] \in \mathbb{R}^{d \times n}$ is the data matrix, $U \in \mathbb{R}^{n \times c}$ is the membership degree matrix, and $B \in \mathbb{R}^{c \times c}$ is a diagonal matrix with the k -th diagonal element being $b_{kk} = 1 / \sum_{i=1}^n u_{ik}$. To concentrate on the main idea, **the proof for Eq. (11) is moved to the Appendix.**

According to the graph theory proposed by Liu et al. [41], we know that the matrix $I_n - UBU^T$ in Eq. (11) can be a Laplacian matrix on the anchor graph, and the corresponding adjacency matrix is $\{\hat{W} | \hat{w}_{ij} = \sum_{k=1}^c u_{ik} u_{jk} / b_{kk}\}$. Then we can conclude that

$$\text{Tr} [X(I_n - UBU^T)X^T] = \frac{1}{2} \sum_{i=1}^n \sum_{j=1}^n \hat{w}_{ij} \|x_i - x_j\|_2^2 \quad (12)$$

where \hat{w}_{ij} reflects the relationship between x_i and x_j . Therefore, if we consider data matrix X as a variable and denote it by \tilde{X} , it is possible to project the data into a new manifold by optimizing the following objective function.

$$\min_{\tilde{X}} \text{Tr} [\tilde{X}(I_n - UBU^T)\tilde{X}^T] \quad (13)$$

where $\tilde{X} \in \mathbb{R}^{\tilde{d} \times n}$ denotes the newly learned data matrix, and \tilde{d} denotes the dimension of the newly learned sample \tilde{x}_i . Utilizing the objective function in Eq. (13) can make the projected data more compact within the same cluster, but sometimes the learned Laplacian matrix $I_n - UBU^T$ may be inaccurate and lead to incorrect projection. Therefore, we attempt to introduce the normalized Laplacian matrix \hat{L} (see the definition in Notations) into the objective function in Eq. (13) to help obtain a better manifold. The specific formulation is given as follows.

$$\min_{\tilde{X}} \text{Tr} [\tilde{X}(I_n - UBU^T)\tilde{X}^T] + \lambda \text{Tr}(\tilde{X}\hat{L}\tilde{X}^T) \quad (14)$$

where $\lambda \in \mathbb{R}^+$ is used to balance the influence of the second term. Then, **the objective function of the proposed AFCM (Adaptive Fuzzy C-Means with graph embedding) model is shown as follows.**

$$\begin{aligned} \min_{U, V, \gamma, \tilde{X}} \sum_{i=1}^n \sum_{j=1}^c u_{ij} \gamma \|\tilde{x}_i - v_j\|_2^2 + \lambda \text{Tr}(\tilde{X}\hat{L}\tilde{X}^T) \\ + u_{ij} \log u_{ij} - n \log \gamma^{\frac{d}{2}}, \\ \text{s.t.} \quad \tilde{X}\tilde{X}^T = I_{\tilde{d}}, \quad \sum_{j=1}^c u_{ij} = 1, \quad 0 < u_{ij} < 1 \end{aligned} \quad (15)$$

where \tilde{d} is the dimension of the projected sample \tilde{x}_i , and in this paper we directly set $\tilde{x}_i = c$, and the orthogonal constraint $\tilde{X}\tilde{X}^T = I_{\tilde{d}}$ is introduced to avoid trivial solutions. Note that the model in Eq. (10) can be viewed as a degenerate form of the proposed model in Eq. (15).

B. Optimization

There are four variables to be updated for the proposed objective function in Eq. (15).

When we update U while keeping other variables fixed, the objective function in Eq. (15) can be reformulated as

$$\begin{aligned} \min_U \sum_{i=1}^n \sum_{j=1}^c u_{ij} \gamma \|\tilde{x}_i - v_j\|_2^2 + u_{ij} \log(u_{ij}) \\ \text{s.t. } \sum_{j=1}^c u_{ij} = 1, \quad 0 < u_{ij} < 1 \end{aligned} \quad (16)$$

An usual way to solve problem in Eq. (16) is using the Lagrange multiplier method [42]. The Lagrange function is given as

$$\begin{aligned} L(U, \eta) = \sum_{i=1}^n \sum_{j=1}^c u_{ij} \gamma \|\tilde{x}_i - v_j\|_2^2 \\ + u_{ij} \log(u_{ij}) + \sum_{i=1}^n \eta_i \left(\sum_{j=1}^c u_{ij} - 1 \right) \end{aligned} \quad (17)$$

By setting the derivative of the Lagrange function to zero with respect to u_{ij} , and combining it with the constraint $\sum_{j=1}^c u_{ij} = 1$, we obtain the update solution of u_{ij} as follows.

$$u_{ij} = \frac{\exp\{-\gamma \|\tilde{x}_i - v_j\|_2^2\}}{\sum_{j=1}^c \exp\{-\gamma \|\tilde{x}_i - v_j\|_2^2\}} \quad (18)$$

When we update V while keeping other variables fixed, the objective function in Eq. (15) can be reformulated as

$$\min_V \sum_{i=1}^n \sum_{j=1}^c u_{ij} \|\tilde{x}_i - v_j\|_2^2 \quad (19)$$

By setting the derivative of the objective function in Eq. (19) to zero with respect to v_j we obtain the update equation of v_j as follows.

$$v_j = \frac{\sum_{i=1}^n u_{ij} \tilde{x}_i}{\sum_{i=1}^n u_{ij}} \quad (20)$$

When we update γ while keeping other variables fixed, the objective function in Eq. (15) can be reformulated as

$$\min_{\gamma} \sum_{i=1}^n \sum_{j=1}^c u_{ij} \gamma \|\tilde{x}_i - v_j\|_2^2 - n \log \gamma^{\frac{\tilde{d}}{2}} \quad (21)$$

By setting the derivative of the objective function in Eq. (21) to zero with respect to γ we obtain the update equation of γ as follows.

$$\gamma = \frac{\frac{1}{2} \tilde{d} n}{\sum_{i=1}^n \sum_{j=1}^c u_{ij} \|\tilde{x}_i - v_j\|_2^2} \quad (22)$$

Algorithm 1 Algorithm for AFCM in Eq. (15)

- 1: **Input:** Data matrix X , cluster number c , parameter λ , and normalized Laplacian matrix \hat{L} .
 - 2: **Initialization:** Membership degree matrix U , cluster center V , adaptive hyper-parameter γ and projected dimension $\tilde{d} = c$.
 - 3: **while** not converge **do**
 - 4: $\tilde{X} \leftarrow$ eigenvector $[\gamma(I_n - UDU^T) + \lambda \hat{L}]$, c smallest vectors];
 - 5: Update v_j by Eq. (20);
 - 6: Update γ by Eq. (22);
 - 7: Update u_{ij} by Eq. (18);
 - 8: **end while**
 - 9: **Output:** membership degree matrix U .
-

Algorithm 2 Algorithm for degenerated AFCM in Eq. (10)

- 1: **Input:** Data matrix X and cluster number c .
 - 2: **Initialization:** Membership degree matrix U , projected data matrix $\tilde{X} = X$ and projected dimension $\tilde{d} = d$.
 - 3: **while** not converge **do**
 - 4: Update v_j by Eq. (20);
 - 5: Update γ by Eq. (22);
 - 6: Update u_{ij} by Eq. (18);
 - 7: **end while**
 - 8: **Output:** membership degree matrix U .
-

When we update \tilde{X} while keeping other variables fixed, the objective function in Eq. (15) can be reformulated as

$$\begin{aligned} \min_{\tilde{X}} \sum_{i=1}^n \sum_{j=1}^c u_{ij} \gamma \|\tilde{x}_i - v_j\|_2^2 + \lambda \text{Tr}(\tilde{X} \hat{L} \tilde{X}^T) \\ \Leftrightarrow \min_{\tilde{X}} \gamma \text{Tr} \left[\tilde{X} (I_n - UBU^T) \tilde{X}^T \right] + \lambda \text{Tr}(\tilde{X} \hat{L} \tilde{X}^T) \quad (23) \\ \Leftrightarrow \min_{\tilde{X}} \text{Tr} \left\{ \tilde{X} \left[\gamma (I_n - UBU^T) + \lambda \hat{L} \right] \tilde{X}^T \right\} \\ \text{s.t. } \tilde{X} \tilde{X}^T = I_{\tilde{d}} \end{aligned}$$

The proof for Eq. (23) is similar to that for Eq. (11), which has been provided in the Appendix. According to the Rayleigh quotient [43], the problem in Eq. (23) can be solved by selecting the c minimum eigenvectors of matrix $\gamma(I_n - UBU^T) + \lambda \hat{L}$.

Up to this point, the optimization process has been completed. Algorithm 1 presents the pseudo code for optimizing the AFCM model defined in Eq. (15). Algorithm 2 presents the pseudo code for optimizing the degenerate AFCM model defined in Eq. (10).

C. Construction of the Affinity Matrix

For graph embedded methods, it is important to construct a proper affinity matrix. In this paper, we use the Gaussian kernel to construct the affinity matrix as follows.

$$w_{ij} = \begin{cases} \exp\left(-\frac{\|\mathbf{x}_i - \mathbf{x}_j\|_2^2}{2\sigma^2}\right) & \text{if } x_j \in \mathcal{N}(x_i) \\ 0, & \text{otherwise} \end{cases} \quad (24)$$

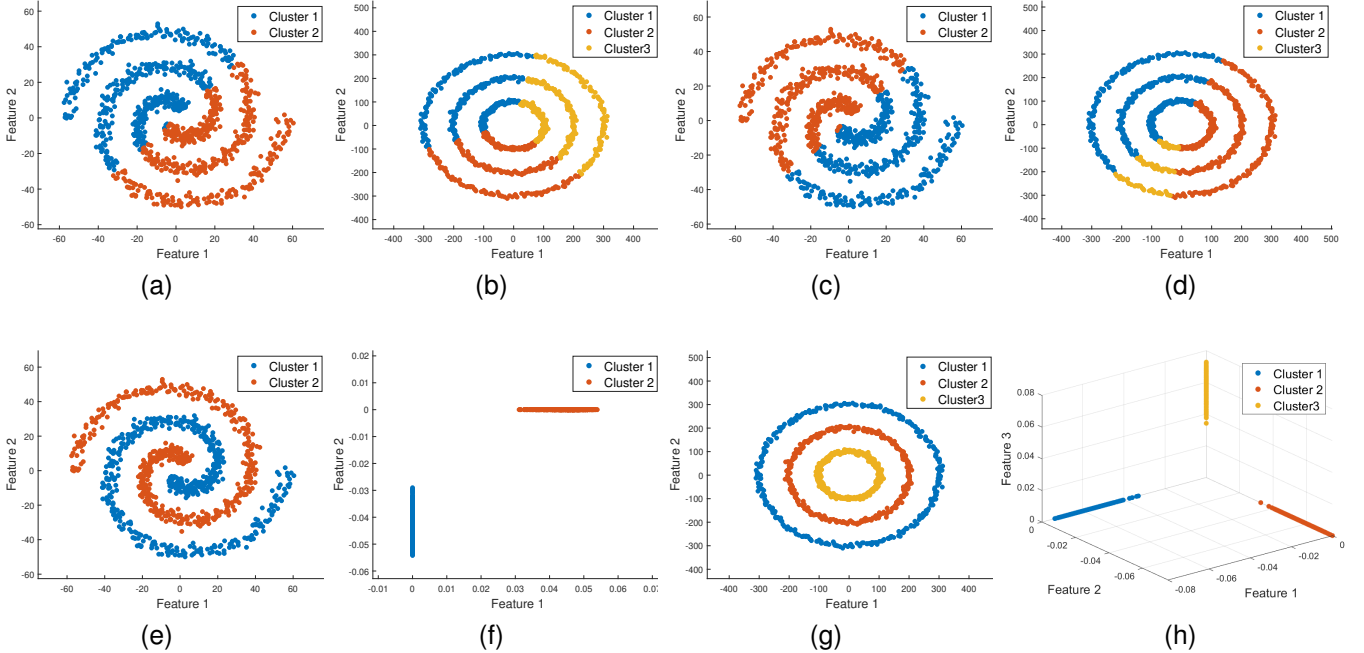


Fig. 2. Clustering results on toy datasets. (a) and (b) depict the clustering outcomes of FCM. (c) and (d) show the clustering results of degenerate AFCM. (e)-(h) present the clustering results of AFCM, which projects data from the original manifold into a newly learned manifold and perform clustering in this new manifold rather than the original manifold.

where σ is a predefined scalar, $\mathcal{N}(x_i)$ denotes the set of the k nearest neighbour of x_i . In this paper, we set the value of $\sigma = 2$.

D. Computational Complexity Analysis

Let n represent the number of samples, c represent the number of clusters, d and \bar{d} represent the original dimension and the projected dimension, and t represent the number of iterative steps. For Algorithm 1, in each iterative step, the computational complexity of updating U is $\mathcal{O}(nc\bar{d})$, which is the same as that of updating V and γ . Then the computational complexity of updating \tilde{X} focuses on performing eigenvalue decomposition, which is $\mathcal{O}(n^3)$. Therefore, the overall computational complexity of the proposed AFCM method in Algorithm 1 is $\mathcal{O}(tn^3 + 3tnc\bar{d})$, which can be simplified to $\mathcal{O}(tn^3)$. For Algorithm 2, since \tilde{X} is not updated, the algorithm operates in the original dimension d , resulting in a total computational complexity of $\mathcal{O}(tncd)$.

TABLE I
DESCRIPTION OF DATA SETS.

Data set	Samples	Dimensions	Clusters
Iris	150	4	3
Breast	699	10	2
Vehicle	846	18	4
UPPS	1854	256	10
Jaffe50	213	1024	10
warpPIE10P	210	2420	10
Olivetti	900	2500	10
ORL64x64	400	4096	40
Pose07	1629	4096	68
Pose29	1632	4096	68

IV. EXPERIMENT

A. Description of Datasets

In this subsection, we provide a description of the experimental datasets. Ten real-world datasets are used in experiments, including Iris¹, Breast¹, Vehicle¹, USPS², Jaffe50³, warpPIE10P⁴, Olivetti¹, ORL64x64², Pose07⁵, and Pose29⁵. The details of these real-world datasets are given in Table I.

B. Experimental Settings

In this experiment, seven state-of-the-art clustering algorithms are selected as the comparative algorithms to be compared with the proposed AFCM algorithm. These comparative algorithms include Fuzzy C-Means (FCM) [1], Fuzzy C-Means with Entropy Regularization (FCM-ER) [3], Spectral Clustering (SC) [18], Robust Sparse Fuzzy K-Means (RSFKM) [5], Coordinate Descent K-Means (CDKM) [44], Fuzzy K-Means with Pattern Shrinking (FKPS) [28] and Fast Clustering model with Anchor Guidance (FCAG) [22].

To ensure a consistent standardization of the data, each dataset is subjected to normalization using the min-max normalization method. For fair comparison with the competitors, based on their given parameter lists, we use the grid-search method to select the best parameter values for each comparative algorithm. There are two parameters in the proposed AFCM algorithm including the number of the

¹<https://archive.ics.uci.edu>

²<http://www.cad.zju.edu.cn/home/dengcai/Data/MLData.html>

³<https://www.kaggle.com/>

⁴<https://jundongl.github.io/scikit-feature/datasets.html>

⁵<https://www.ri.cmu.edu/publications/the-cmu-pose-illumination-and-expression-pie-database/>

TABLE II
CLUSTERING RESULTS FOR AFCM ON TEN REAL-WORLD DATA SETS (AVERAGE ACC, NMI AND ARI \pm STANDARD DEVIATIONS $\times 1E+2$). THE BOLD CHARACTERS ARE THE OPTIMAL RESULTS.

Dataset	Metric	FCM	FCM-ER	SC	RSFKM	CDKM	FKPS	FCAG	AFCM
Iris	ACC	88.73(± 0.20)	89.33(± 0.00)	94.67(± 0.00)	88.67(± 0.00)	88.67(± 2.58)	92.00(± 0.00)	95.47(± 2.40)	96.13(± 1.60)
	NMI	73.01(± 0.37)	73.64(± 0.00)	85.88(± 0.00)	75.48(± 0.63)	73.64(± 0.00)	79.82(± 0.00)	86.32(± 3.36)	87.49(± 2.89)
	ARI	71.64(± 0.41)	72.78(± 0.00)	78.29(± 0.02)	75.60(± 0.00)	71.63(± 0.00)	78.74(± 0.00)	87.48(± 5.78)	89.07(± 3.93)
Breast	ACC	94.99(± 0.00)	96.28(± 0.00)	96.04(± 0.00)	95.28(± 0.00)	95.28(± 0.00)	96.28(± 0.00)	95.99(± 0.00)	96.57(± 0.00)
	NMI	69.15(± 0.00)	75.60(± 0.00)	74.36(± 4.55)	70.53(± 0.00)	70.49(± 0.00)	75.76(± 0.00)	74.17(± 0.00)	78.00(± 0.00)
	ARI	80.74(± 0.28)	85.54(± 0.15)	84.63(± 0.00)	81.79(± 0.00)	81.79(± 0.00)	85.60(± 0.00)	84.46(± 0.00)	86.64(± 0.00)
Vehicle	ACC	37.12(± 0.13)	36.90(± 0.51)	41.80(± 0.57)	38.09(± 1.69)	36.87(± 0.52)	38.75(± 0.76)	42.08(± 3.56)	46.74(± 2.83)
	NMI	10.53(± 1.58)	10.60(± 1.70)	16.15(± 2.42)	10.59(± 0.75)	10.59(± 1.71)	11.79(± 2.76)	14.63(± 4.44)	19.81(± 1.82)
	ARI	7.86(± 0.83)	8.36(± 0.21)	11.15(± 0.01)	9.11(± 0.37)	7.88(± 0.87)	8.55(± 0.00)	11.17(± 2.27)	15.75(± 2.25)
USPS	ACC	65.78(± 1.56)	64.53(± 1.42)	69.32(± 2.48)	66.04(± 3.59)	66.59(± 2.67)	66.42(± 2.28)	74.02(± 2.48)	72.07(± 4.32)
	NMI	62.91(± 0.91)	62.72(± 0.04)	73.61(± 1.52)	64.00(± 1.33)	62.67(± 1.28)	63.80(± 1.60)	71.17(± 1.08)	77.59(± 1.58)
	ARI	54.11(± 1.38)	53.53(± 1.32)	62.83(± 2.99)	55.04(± 3.13)	53.94(± 1.79)	55.27(± 2.00)	62.85(± 1.15)	65.67(± 4.21)
Jaffe50	ACC	92.77(± 0.00)	84.55(± 3.30)	86.43(± 2.96)	86.90(± 3.60)	77.65(± 6.64)	42.18(± 2.46)	89.95(± 3.57)	94.93(± 3.86)
	NMI	92.27(± 0.00)	89.75(± 2.70)	90.38(± 1.34)	89.47(± 2.76)	85.76(± 3.28)	48.00(± 2.77)	92.33(± 2.14)	95.20(± 2.15)
	ARI	85.88(± 0.00)	79.78(± 5.15)	82.09(± 0.00)	79.67(± 2.50)	72.09(± 6.00)	49.09(± 2.87)	84.96(± 4.589)	91.23(± 4.26)
warpPIE10P	ACC	28.24(± 1.76)	62.00(± 5.52)	48.48(± 1.62)	27.95(± 1.15)	28.52(± 1.29)	29.33(± 1.78)	44.00(± 3.42)	50.57(± 0.29)
	NMI	30.06(± 2.13)	29.91(± 3.49)	61.05(± 2.81)	30.07(± 1.67)	31.01(± 1.63)	31.65(± 2.75)	52.06(± 3.05)	63.79(± 0.86)
	ARI	9.53(± 1.98)	9.16(± 1.27)	35.80(± 3.77)	9.27(± 1.27)	9.85(± 1.46)	10.67(± 1.45)	26.81(± 3.45)	39.11(± 1.02)
Olivetti	ACC	53.88(± 3.24)	49.76(± 3.18)	68.56(± 0.00)	51.03(± 3.47)	47.10(± 3.20)	51.90(± 5.01)	59.11(± 2.55)	70.41(± 2.89)
	NMI	52.10(± 2.38)	50.98(± 3.66)	71.88(± 0.37)	51.89(± 1.94)	50.93(± 2.84)	53.75(± 3.78)	60.71(± 4.49)	74.98(± 1.68)
	ARI	36.92(± 2.61)	33.45(± 2.89)	50.66(± 1.06)	34.82(± 2.09)	33.32(± 2.72)	36.19(± 3.60)	43.56(± 5.48)	59.92(± 2.23)
ORL64x64	ACC	59.40(± 1.39)	57.98(± 1.65)	58.55(± 2.36)	58.68(± 2.44)	58.10(± 2.79)	58.58(± 2.22)	62.38(± 1.35)	62.90(± 2.65)
	NMI	77.63(± 0.99)	77.46(± 0.79)	77.69(± 1.94)	77.67(± 0.88)	76.82(± 1.38)	77.74(± 1.02)	81.75(± 0.88)	80.68(± 0.46)
	ARI	46.00(± 1.25)	45.29(± 2.05)	41.64(± 5.30)	45.956(± 2.20)	44.09(± 2.82)	46.10(± 1.97)	53.94(± 2.14)	50.94(± 1.58)
Pose07	ACC	15.95(± 0.44)	15.49(± 0.27)	28.86(± 0.83)	15.02(± 0.34)	16.24(± 0.67)	15.43(± 0.48)	23.20(± 0.77)	32.42(± 1.07)
	NMI	42.86(± 0.36)	42.28(± 0.22)	53.54(± 1.24)	42.04(± 0.45)	42.23(± 0.64)	42.10(± 0.48)	54.34(± 0.43)	60.54(± 0.62)
	ARI	8.80(± 0.31)	5.84(± 0.22)	11.26(± 1.24)	5.25(± 0.21)	5.84(± 0.44)	5.49(± 0.37)	12.52(± 0.54)	18.58(± 1.31)
Pose29	ACC	17.12(± 0.29)	15.40(± 0.37)	26.65(± 0.42)	15.92(± 0.55)	17.46(± 0.53)	15.70(± 0.43)	25.03(± 0.65)	32.61(± 1.85)
	NMI	44.01(± 0.47)	42.72(± 0.63)	43.49(± 2.01)	43.59(± 0.31)	42.25(± 0.64)	41.35(± 0.47)	55.69(± 0.30)	59.15(± 1.11)
	ARI	6.89(± 0.25)	6.05(± 0.32)	4.69(± 1.10)	6.21(± 0.33)	6.36(± 0.44)	5.72(± 0.38)	13.98(± 0.38)	17.51(± 1.46)

nearest neighbors k in the normalized Laplacian matrix and the regularization parameter λ , and their parameter lists are given as [3, 4, 5, 6, 8, 10, 12] and [1e-1, 1e1, 1e2, 1e3, 1e4, 1e5, 1e6], respectively. Similar to the competitors, we also use the grid-search method to select parameters for AFCM. Accuracy (ACC), Normalized Mutual Information (NMI), and Adjusted Rand Index (ARI) are three commonly utilized metrics for assessing the performance of clustering algorithms [45], and they are employed in our paper as well.

C. Visualization Experiments on Toy Datasets

We conduct visualization experiments on two synthetic toy datasets to demonstrate the capability of the proposed model on handling data with non-Gaussian clusters. The first one consists of two spiral-shaped clusters, with each cluster containing 500 samples. The second one consists of three ring-shaped clusters, with each cluster containing 300 samples.

First, we perform FCM on the toy datasets and the clustering results are shown in Fig. 2a and Fig. 2b. Obviously, FCM cannot handle this type of data. Then, we show the clustering results of the degenerate AFCM in Fig. 2c and Fig. 2d. Since the degenerate AFCM performs clustering directly in the original manifold, it consequently fails as well. Finally, we present the clustering results of the proposed AFCM that performs

clustering in the learned manifold. In Fig. 2e and Fig. 2g, we show the clustering results of AFCM in the original manifold. In Fig. 2f and Fig. 2h, we show the clustering results of AFCM in the learned manifold. By observing the clustering results, it is clear that the proposed AFCM successfully projected the data from a non-Gaussian manifold into a Gaussian manifold, and then successfully clustered the data.

D. Evaluation on Real-World Datasets

In order to further verify the effectiveness of the proposed AFCM method, we compare it with seven state-of-the-art clustering methods on ten real-world datasets. To ensure a fair comparison, we execute each algorithm ten times and present the average results along with standard deviations. The clustering outcomes are evaluated using three frequently used metrics: ACC, NMI, and ARI. The clustering results are shown in Table II.

According to the clustering results in Table II, the proposed AFCM obtains the optimal results on most datasets, except for the USPS and ORL64x64 datasets. The comparative algorithm FCAG exhibits better performance than the proposed AFCM on the USPS in terms of ACC, but AFCM outperforms FCAG in terms of NMI and ARI on the same dataset. A similar situation also occurs with the ORL64x64 dataset. Therefore,

TABLE III
CLUSTERING RESULTS FOR THE ABLATION EXPERIMENTS ON EIGHT REAL-WORLD DATA SETS (AVERAGE ACC, NMI AND ARI \pm STANDARD DEVIATIONS $\times 1E+2$). THE BOLD CHARACTERS ARE THE OPTIMAL RESULTS. ABLATION-1 AND ABLATION-2 ADOPT THE TWO-STAGE STRATEGY, WHEREAS AFCM TAKES THE ONE-STAGE STRATEGY.

Metric	Method	Iris	Breast	Vehicle	USPS	warpPIE10P	Olivetti	ORL64x64	Pose07
ACC	Ablation-1	94.67(± 0.00)	95.85(± 0.00)	41.76(± 0.46)	69.31(± 3.34)	47.52(± 2.65)	67.69(± 0.16)	59.45(± 1.83)	27.26(± 1.38)
	Ablation-2	94.67(± 0.00)	95.85(± 0.00)	44.65(± 2.51)	71.65(± 3.89)	50.29(± 0.32)	68.54(± 2.10)	61.63(± 1.93)	31.33(± 1.05)
	AFCM	96.13(± 1.60)	96.57(± 0.00)	46.74(± 2.83)	72.07(± 4.32)	50.57(± 0.29)	70.41(± 2.89)	62.90(± 2.65)	32.42(± 1.07)
NMI	Ablation-1	85.88(± 0.00)	73.45(± 0.00)	16.08(± 0.00)	75.04(± 2.46)	58.90(± 3.17)	70.69(± 1.59)	76.98(± 1.62)	52.64(± 1.84)
	Ablation-2	85.88(± 0.00)	73.45(± 0.00)	18.01(± 1.21)	76.39(± 2.43)	62.52(± 1.27)	71.72(± 2.82)	80.72(± 0.78)	59.93(± 0.76)
	AFCM	87.49(± 2.89)	78.00(± 0.00)	19.81(± 1.82)	77.59(± 1.58)	63.79(± 0.86)	74.98(± 1.68)	80.68(± 0.46)	60.54(± 0.62)
ARI	Ablation-1	85.15(± 0.00)	83.94(± 0.00)	10.86(± 0.00)	61.85(± 5.43)	32.04(± 3.28)	48.86(± 1.45)	40.89(± 3.19)	10.84(± 1.40)
	Ablation-2	85.15(± 0.00)	83.94(± 0.00)	14.34(± 2.01)	64.00(± 5.42)	37.59(± 1.40)	56.75(± 3.82)	50.41(± 1.65)	16.76(± 1.59)
	AFCM	89.07(± 3.93)	86.64(± 0.00)	15.75(± 2.25)	66.57(± 4.21)	39.11(± 1.02)	59.92(± 2.23)	50.94(± 1.58)	18.58(± 1.31)

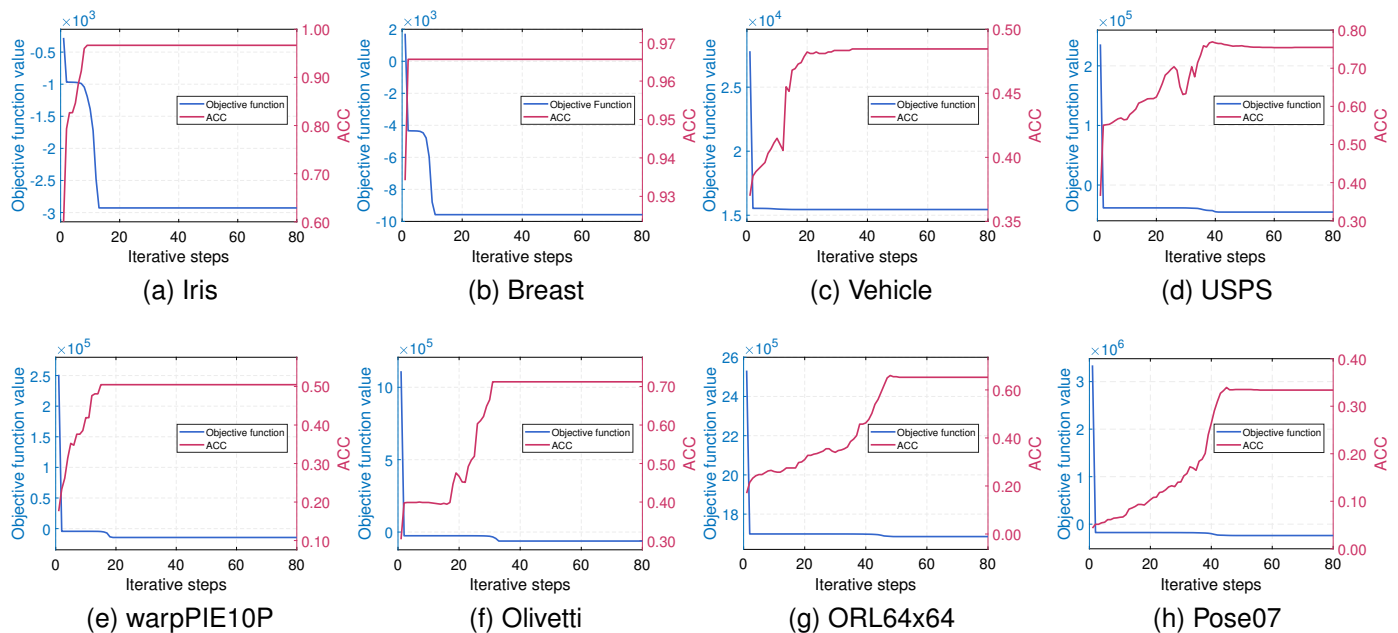


Fig. 3. Convergence and ACC curves for AFCM on eight real-world datasets.

while the performance of AFCM is comparable to FCAG on the USPS and ORL64x64 datasets, it obtains the best clustering results on the other eight datasets, validating the effectiveness of the proposed AFCM method. Moreover, it is observed that the graph based method AFCM, SC, and FCAG usually perform better than other non-graph based methods. This observation indicates that graph embedding is an excellent method to help improve clustering performance.

E. Ablation Experiments

In this subsection, we want to verify two facts through the ablation experiment. The first one is that the parameter-free degenerate AFCM algorithm can be an excellent alternative to K-Means. The second one is that simultaneously performing clustering and manifold learning may obtain better results than performing them separately.

To verify this, we construct two comparative algorithms named as Ablation-1 and Ablation-2. Ablation-1 is a two-stage method, which first computes the c minimum eigenvectors

of the normalized Laplacian matrix \hat{L} and then performs K-Means on these eigenvectors. Ablation-2 is also a two-stage method, which first computes the c minimum eigenvectors of the normalized Laplacian matrix \hat{L} and then performs the degenerate AFCM on the eigenvectors. We run each algorithm ten times, recording the average clustering results, which are presented in Table III.

According to the results in Table III, it is observed that the performance of Ablation-2 is better than that of Ablation-1, which means that the performance of the degenerate AFCM is better than K-means. The degenerate AFCM has the similar computational complexity with K-Means but exhibit a better performance than K-Means. Therefore it is an excellent alternative to K-means. Furthermore, the performance of the one-stage method AFCM is better than Ablation-1 and Ablation-2 that adopts two-stage approaches, which means perform clustering and manifold learning together is better than performing them separately.

F. Convergence Experiments

In order to validate the convergence of the proposed AFCM algorithm, we present the curves of the objective function values and the ACC values in Figure 3. The experiment was conducted using eight real-world datasets, with the maximum number of iterations set to 80.

From the results depicted in Figure 3, it is evident that the curves of the objective function values for all eight datasets exhibit a monotonically decreasing trend. This observation confirms the efficacy of the optimization strategy employed in the AFCM model. Additionally, the ACC curves in Figure 3 show a general trend of increasing with the iterative steps, albeit not strictly monotonic. There are instances where the ACC values may decrease temporarily; however, upon convergence, the ACC values significantly surpass those at the initial iterative step. This pattern validates the rationality and effectiveness of the proposed AFCM model design.

Overall, the experimental results presented in Figure 3 demonstrate the successful convergence and effectiveness of the AFCM algorithm across diverse real-world datasets.

V. CONCLUSIONS

In this paper, we propose a novel Adaptive Fuzzy C-Means with graph embedding model (AFCM) that can automatically learn the membership degree hyper-parameter and handle data with non-Gaussian clusters. By establishing the equivalent connections between FCM with entropy regularization and the generalized Gaussian mixture model, we reveal that the entropy regularization hyper-parameter in FCM can be interpreted as the scale parameter in the generalized Gaussian mixture model. Therefore, the entropy regularization hyper-parameter can be learned in a similar way to the scale parameter in the mixture model. Furthermore, by introducing the graph embedding regularization, the proposed AFCM model is capable of handling data with non-Gaussian clusters. Note that, the proposed method perform clustering and manifold learning simultaneously, which is better than performing them separately, and we validate this by experiments. Moreover, the proposed AFCM can degenerate into a parameter-free FCM. This simplified AFCM variant maintains a computational complexity of $\mathcal{O}(ncd)$, comparable to K-Means, yet outperforms K-Means in performance. However, while the proposed AFCM achieves good performance, it still relies on the original FCM to conduct clustering in the newly learned manifold. In the future, we aim to integrate more advanced techniques into AFCM to enhance its clustering performance in the new manifold.

APPENDIX

PROOF FOR PROPOSITION 1

In this section, we presents a rigorous mathematical proof of Proposition 1. To facilitate the readers, we rewritten the

equivalent objective function of the generalized Gaussian mixture model as follows.

$$\begin{aligned} \min_{U, \alpha, V, \Sigma, \beta, m} \sum_{i=1}^n \sum_{j=1}^c u_{ij} \left\{ m \left[(x_i - v_j)^T \Sigma_j^{-1} (x_i - v_j) \right]^\beta \right. \\ \left. + \frac{1}{2} \log |\Sigma_j| - \log \alpha_j - \log \frac{\beta \Gamma(\frac{d}{2}) m^{\frac{d}{2\beta}}}{\pi^{\frac{d}{2}} \Gamma(\frac{d}{2\beta})} + \log u_{ij} \right\}, \end{aligned} \quad (25)$$

$$\text{s.t. } \sum_{j=1}^c \alpha_j = 1, \quad 0 < \alpha_j < 1,$$

$$\sum_{j=1}^c u_{ij} = 1, \quad 0 < u_{ij} < 1$$

where u_{ij} is the membership degree denoting the probability of sample x_i being assigned to the j -th cluster, $\alpha = \{\alpha_1, \alpha_2, \dots, \alpha_c\}$, $V = \{v_1, v_2, \dots, v_c\}$ and $\Sigma = \{\Sigma_1, \Sigma_2, \dots, \Sigma_c\}$, denote the sets of mixing coefficients, means and scale matrices, and β and m denotes the shape parameter and the scale parameter in the generalized Gaussian mixture model.

We will demonstrate that the update equations for the equivalent objective function outlined in Eq. (25) coincide with those derived for the log-likelihood function of the generalized Gaussian mixture model.

A. The maximum log-likelihood function

Let $x \in \mathbb{R}^d$ be a d -dimensional random vector, and the probability density function of the generalized Gaussian distribution is given as below.

$$g(x|\theta) = \frac{\beta \Gamma(\frac{d}{2}) m^{\frac{d}{2\beta}}}{\pi^{\frac{d}{2}} \Gamma(\frac{d}{2\beta})} |\Sigma|^{-\frac{1}{2}} \exp \left\{ -m \left[(x-v)^T \Sigma^{-1} (x-v) \right]^\beta \right\} \quad (26)$$

where $\theta = \{v, \Sigma, \beta, m\}$ denotes the set of parameters, $v \in \mathbb{R}^d$ denotes the mean, $\Sigma \in \mathbb{R}^{d \times d}$ denotes the positive definite covariance matrix, $\beta \in \mathbb{R}^+$ denotes the shape parameter, and m denotes the scale parameter.

Based on the probability density function the generalized Gaussian distribution depicted in Eq. (26), the probability density function of the generalized Gaussian mixture model can be defined as

$$f(x|\Theta) = \sum_{j=1}^c \alpha_j g(x|\theta_j), \quad \text{s.t. } \sum_{j=1}^c \alpha_j = 1 \quad (27)$$

where $\Theta = \{\alpha, V, \Sigma, \beta, m\}$ denotes the set of all parameters in the generalized Gaussian mixture model, $\theta_j = \{v_j, \Sigma_j, \beta, m\}$ denotes the parameter set of the j -th component, $\alpha = \{\alpha_1, \alpha_2, \dots, \alpha_c\}$ denotes the set of mixing coefficients, and c denotes the number of components.

Then the expression of the log-likelihood function for the generalized Gaussian mixture model is presented as follows.

$$\begin{aligned} L(\Theta|X) = \sum_{i=1}^n \log f(x_i|\Theta) = \sum_{i=1}^n \log \sum_{j=1}^c \alpha_j g(x_i|\theta_j), \\ \text{s.t. } \sum_{j=1}^c \alpha_j = 1 \end{aligned} \quad (28)$$

B. EM for problem in (28)

Owing to the combination of logarithm and sum within the problem depicted in Eq. (28), direct optimization becomes challenging, necessitating the utilization of the EM algorithm. There are two main steps in the EM, including E-step and M-step.

In E-step: According to the log-likelihood function in Eq. (28) one has

$$\begin{aligned} p(j|x_i, \Theta^{t-1}) &= \frac{\alpha_j^{t-1} g(x_i|\theta_j^{t-1})}{\sum_{j=1}^c \alpha_j^{t-1} g(x_i|\theta_j^{t-1})} \\ &= \frac{\alpha_j^{t-1} |\Sigma_j^{t-1}|^{-\frac{1}{2}} \exp\{-m^{t-1}(d_{ij})^{t-1}\}}{\sum_{j=1}^c \alpha_j^{t-1} |\Sigma_j^{t-1}|^{-\frac{1}{2}} \exp\{-m^{t-1}(d_{ij})^{t-1}\}} \end{aligned} \quad (29)$$

where $(d_{ij})^{t-1} = \left[(x_i - v_j^{t-1})^T (\Sigma_j^{t-1})^{-1} (x_i - v_j^{t-1}) \right]^{\beta^{t-1}}$; symbols Θ^{t-1} and θ_j^{t-1} denote the parameter sets estimated in last iteration, and $p(j|x_i, \Theta^{t-1})$ can be considered as the posterior probability of the i -th sample being generated by the j -th mixture component.

In M-step: Fix $p(j|x_i, \Theta^{t-1})$ and optimize the following problem.

$$\begin{aligned} \max_{\Theta} Q(\Theta, \Theta^{t-1}) &= \max_{\Theta} \sum_{i=1}^n \sum_{j=1}^c p(j|x_i, \Theta^{t-1}) \log \alpha_j g(x_i|\theta_j) \\ &= \max_{\Theta} \sum_{i=1}^n \sum_{j=1}^c p(j|x_i, \Theta^{t-1}) \log \left\{ \alpha_j \frac{\beta \Gamma(\frac{d}{2}) m^{\frac{d}{2\beta}}}{\pi^{\frac{d}{2}} \Gamma(\frac{d}{2\beta})} \times \right. \\ &\quad \left. |\Sigma_j|^{-\frac{1}{2}} \exp \left[-m \left((x_i - v_j)^T \Sigma_j^{-1} (x_i - v_j) \right)^{\beta} \right] \right\} \\ \Leftrightarrow \min_{\Theta} \sum_{i=1}^n \sum_{j=1}^c p(j|x_i, \Theta^{t-1}) &\left\{ m \left[(x_i - v_j)^T \Sigma_j^{-1} (x_i - v_j) \right]^{\beta} \right. \\ &\quad \left. + \frac{1}{2} \log |\Sigma_j| - \log \alpha_j - \log \frac{\beta \Gamma(\frac{d}{2}) m^{\frac{d}{2\beta}}}{\pi^{\frac{d}{2}} \Gamma(\frac{d}{2\beta})} \right\} \\ \text{s.t. } \sum_{j=1}^c \alpha_j &= 1, \quad 0 < \alpha_j < 1, \end{aligned} \quad (30)$$

where $\Theta = \{\alpha, V, \Sigma, \beta, m\}$.

Through iterative execution of the E-step and M-step until converging, one can obtain a suitable local minimum for the log-likelihood function presented in Eq. (28).

C. Proof for equivalence

The proof for the equivalence between the objective function in Eq. (25) and the log-likelihood function in Eq. (28) is mainly divided into two parts. In the first part, we prove that u_{ij} in Eq. (25) have the same update equation with $p(j|x_i, \Theta^{t-1})$ in Eq. (29), where u_{ij} denotes the membership degree and $p(j|x_i, \Theta^{t-1})$ is the posterior probability derived from the E-step. In the second part, we prove that the equivalent objective function in Eq. (25) with U being fixed has the same form with the Q function in Eq. (30).

In the first part: When we update U with the other variables being fixed, the objective function in Eq. (25) can be reformulated as follows.

$$\begin{aligned} \min_U \sum_{i=1}^n \sum_{j=1}^c u_{ij} &\left\{ m \left[(x_i - v_j)^T \Sigma_j^{-1} (x_i - v_j) \right]^{\beta} \right. \\ &\quad \left. + \frac{1}{2} \log |\Sigma_j| - \log \alpha_j + \log u_{ij} \right\}, \quad (31) \\ \text{s.t. } \sum_{j=1}^c u_{ij} &= 1, \quad 0 < u_{ij} < 1 \end{aligned}$$

We remove the inequality constraints and take the Lagrange multiplier method to optimize the objective function in Eq. (31). The corresponding Lagrange function is constructed as

$$\begin{aligned} L(U, \gamma) &= \sum_{i=1}^n \sum_{j=1}^c u_{ij} \left\{ m \left[(x_i - v_j)^T \Sigma_j^{-1} (x_i - v_j) \right]^{\beta} \right. \\ &\quad \left. + \frac{1}{2} \log |\Sigma_j| - \log \alpha_j + \log u_{ij} \right\} + \sum_{i=1}^n \eta_i \left(\sum_{j=1}^c u_{ij} - 1 \right) \end{aligned} \quad (32)$$

where $\eta = \{\eta_1, \eta_2, \dots, \eta_n\}$ is the set of Lagrange multipliers. By setting the derivative of the Lagrange function in Eq. (32) to zero with respect to u_{ij} we have

$$\begin{aligned} \frac{\partial L(U, \eta)}{\partial u_{ij}} &= m \left[(x_i - v_j)^T \Sigma_j^{-1} (x_i - v_j) \right]^{\beta} \\ &\quad + \frac{1}{2} \log |\Sigma_j| - \log \alpha_j + \log u_{ij} + 1 + \eta_i = 0 \end{aligned} \quad (33)$$

Then according to Eq. (33) we can obtain

$$u_{ij} = \frac{\alpha_j |\Sigma_j|^{-\frac{1}{2}} \exp \left\{ -m \left[(x_i - v_j)^T \Sigma_j^{-1} (x_i - v_j) \right]^{\beta} \right\}}{\exp(1 + \eta_i)} \quad (34)$$

By combining Eq. (34) with the constraint $\sum_{j=1}^c u_{ij} = 1$, we can obtain

$$\begin{aligned} \exp(1 + \eta_i) &= \sum_{j=1}^c \alpha_j |\Sigma_j|^{-\frac{1}{2}} \times \\ &\quad \exp \left\{ -m \left[(x_i - v_j)^T \Sigma_j^{-1} (x_i - v_j) \right]^{\beta} \right\} \end{aligned} \quad (35)$$

Substitute $\exp\{1 + \eta_i\}$ in Eq. (35) back into Eq. (34) and then we can obtain

$$u_{ij} = \frac{\alpha_j |\Sigma_j|^{-\frac{1}{2}} \exp \left\{ -m \left[(x_i - v_j)^T \Sigma_j^{-1} (x_i - v_j) \right]^{\beta} \right\}}{\sum_{j=1}^c \alpha_j |\Sigma_j|^{-\frac{1}{2}} \exp \left\{ -m \left[(x_i - v_j)^T \Sigma_j^{-1} (x_i - v_j) \right]^{\beta} \right\}} \quad (36)$$

The solution of in Eq. (36) satisfies the inequality constraint $0 < u_{ij} < 1$, and hence it is a suitable update equation for u_{ij} . By comparing the update equation of u_{ij} in Eq. (36) and the update equation of $p(j|x_i, \Theta^{t-1})$ in Eq. (29), we can find they have the same form. Therefore, u_{ij} can be seen as an equivalence of $p(j|x_i, \Theta^{t-1})$.

In the second part: When we fix U to update the other variables, the objective function in Eq. (25) can be reformulated as follows.

$$\begin{aligned} \min_{\alpha, V, \Sigma, \beta, m} \sum_{i=1}^n \sum_{j=1}^c u_{ij} \left\{ m \left[(x_i - v_j)^T \Sigma_j^{-1} (x_i - v_j) \right]^\beta \right. \\ \left. + \frac{1}{2} \log |\Sigma_j| - \log \alpha_j - \log \frac{\beta \Gamma(\frac{d}{2}) m^{\frac{d}{2\beta}}}{\pi^{\frac{d}{2}} \Gamma(\frac{d}{2\beta})} \right\}, \quad (37) \\ \text{s.t. } \sum_{j=1}^c \alpha_j = 1, \quad 0 < \alpha_j < 1 \end{aligned}$$

By comparing the objective function in Eq. (37) and the Q function in Eq. (30), it is observed that they have the same form and hence their variables share the same update equations as well.

Up to this point, the proof for the equivalence between the objective function in Eq. (25) and the log-likelihood function in Eq. (28) has been completed.

PROOF FOR EQ. (11)

To facilitate the readers, we first rewrite Eq. (11) as below.

$$\sum_{i=1}^n \sum_{j=1}^c u_{ij} \|x_i - v_j\|_2^2 = \text{Tr} [X(I_n - UBU^T)X^T] \quad (38)$$

where $X = [x_1, x_2, \dots, x_n] \in \mathbb{R}^{d \times n}$ denotes the data matrix, u_{ij} denotes the membership degree satisfying $\sum_{j=1}^c u_{ij} = 1$, and $B \in \mathbb{R}^{c \times c}$ is a diagonal matrix with the k -th diagonal element $b_{kk} = 1 / \sum_{i=1}^n u_{ik}$, and $v \in \mathbb{R}^d$ denotes the j -th cluster center. Moreover, the update equation for v_j is supposed to be

$$v_j = \frac{\sum_{i=1}^n u_{ij} x_i}{\sum_{i=1}^n u_{ij}} = \sum_{i=1}^n \left(\frac{u_{ij}}{\sum_{l=1}^n u_{il}} \right) x_i \quad (39)$$

We define

$$p_{ij} = \frac{u_{ij}}{\left(\sum_{l=1}^n u_{il}\right)}, \quad P_j = \begin{pmatrix} p_{1j} & & 0 \\ & \ddots & \\ 0 & & p_{nj} \end{pmatrix} \in \mathbb{R}^{n \times n} \quad (40)$$

where P_j is a diagonal matrix with the k -th diagonal element being p_{kj} . Then we have

$$v_j = \sum_{i=1}^n p_{ij} x_i \quad (41)$$

Let us now direct the attention to the left-hand side of Eq. (38).

$$\begin{aligned} & \sum_{i=1}^n \sum_{j=1}^c u_{ij} \|x_i - v_j\|_2^2 \\ &= \text{Tr} \left[\sum_{i=1}^n \sum_{j=1}^c u_{ij} (x_i - v_j)(x_i - v_j)^T \right] \\ &= \text{Tr} \left[\sum_{j=1}^c \left(\sum_{l=1}^n u_{lj} \right) \sum_{i=1}^n \frac{u_{ij}}{\left(\sum_{l=1}^n u_{il}\right)} (x_i - v_j)(x_i - v_j)^T \right] \\ &= \text{Tr} \left[\sum_{j=1}^c \left(\sum_{l=1}^n u_{lj} \right) \sum_{i=1}^n p_{ij} (x_i - v_j)(x_i - v_j)^T \right] \quad (42) \end{aligned}$$

According to the definition of p_{ij} and P_j in Eq. (40) and the definition of v_j in Eq. (41), we can further conclude

$$\begin{aligned} & \sum_{i=1}^n p_{ij} (x_i - v_j)(x_i - v_j)^T \\ &= [X(I_n - P_j \mathbf{1} \mathbf{1}^T)] P_j [X(I_n - P_j \mathbf{1} \mathbf{1}^T)]^T \\ &= X(I_n - P_j \mathbf{1} \mathbf{1}^T) P_j (I_n - \mathbf{1} \mathbf{1}^T P_j) X^T \\ &= X(P_j - P_j \mathbf{1} \mathbf{1}^T P_j) (I_n - \mathbf{1} \mathbf{1}^T P_j) X^T \\ &= X(P_j - P_j \mathbf{1} \mathbf{1}^T P_j - P_j \mathbf{1} \mathbf{1}^T P_j + P_j \mathbf{1} \mathbf{1}^T P_j \mathbf{1} \mathbf{1}^T P_j) X^T \\ &= X(P_j - P_j \mathbf{1} \mathbf{1}^T P_j) X^T \quad (43) \end{aligned}$$

where $\mathbf{1} \in \mathbb{R}^{n \times 1}$ is a vector with all elements being equal to 1. Substitute Eq. (43) back into Eq. (42) and then we have

$$\begin{aligned} & \text{Tr} \left[\sum_{j=1}^c \left(\sum_{l=1}^n u_{lj} \right) \sum_{i=1}^n p_{ij} (x_i - v_j)(x_i - v_j)^T \right] \\ &= \text{Tr} \left[\sum_{j=1}^c \left(\sum_{l=1}^n u_{lj} \right) X(P_j - P_j \mathbf{1} \mathbf{1}^T P_j) X^T \right] \\ &= \text{Tr} \left\{ X \left[\sum_{j=1}^c \left(\sum_{l=1}^n u_{lj} \right) P_j - \sum_{j=1}^c \left(\sum_{l=1}^n u_{lj} \right) P_j \mathbf{1} \mathbf{1}^T P_j \right] X^T \right\} \\ &= \text{Tr} [X(I_n - UBU^T)X^T] \quad (44) \end{aligned}$$

where $B \in \mathbb{R}^{c \times c}$ is a diagonal matrix with the definition given as below.

$$B = \begin{pmatrix} \frac{1}{\sum_{l=1}^n u_{l1}} & & 0 \\ & \ddots & \\ 0 & & \frac{1}{\sum_{l=1}^n u_{lc}} \end{pmatrix} \quad (45)$$

Up to this point, the proof for Eq. (11) has been completed.

REFERENCES

- [1] J. C. Bezdek, *Pattern recognition with fuzzy objective function algorithms*. Springer Science & Business Media, 2013.
- [2] J. Xue, F. Nie, R. Wang, and X. Li, "Iteratively reweighted algorithm for fuzzy c -means," *IEEE Transactions on Fuzzy Systems*, vol. 30, no. 10, pp. 4310–4321, 2022.
- [3] R.-P. Li and M. Mukaidono, "A maximum-entropy approach to fuzzy clustering," in *Proceedings of 1995 IEEE International Conference on Fuzzy Systems.*, vol. 4. IEEE, 1995, pp. 2227–2232.
- [4] S. Miyamoto and K. Umayahara, "Fuzzy clustering by quadratic regularization," in *Proceedings of 1998 IEEE International Conference on Fuzzy Systems Proceedings.*, vol. 2. IEEE, 1998, pp. 1394–1399.
- [5] J. Xu, J. Han, K. Xiong, and F. Nie, "Robust and sparse fuzzy k -means clustering," in *Proceedings of the Twenty-Fifth International Joint Conference on Artificial Intelligence, IJCAI-16*, 2016, pp. 2224–2230.
- [6] E. H. Ruspini, J. C. Bezdek, and J. M. Keller, "Fuzzy clustering: A historical perspective," *IEEE Computational Intelligence Magazine*, vol. 14, no. 1, pp. 45–55, 2019.
- [7] X. Zhao, Y. Li, and Q. Zhao, "Mahalanobis distance based on fuzzy clustering algorithm for image segmentation," *Digital Signal Processing*, vol. 43, pp. 8–16, 2015.
- [8] Q. Chen, W. Yu, X. Zhao, F. Nie, and X. Li, "Rooted mahalanobis distance based gustafson-kessel fuzzy c -means," *Information Sciences*, vol. 644, p. 118878, 2023.
- [9] L. Chen, C. P. Chen, and M. Lu, "A multiple-kernel fuzzy c -means algorithm for image segmentation," *IEEE Transactions on Systems, Man, and Cybernetics, Part B (Cybernetics)*, vol. 41, no. 5, pp. 1263–1274, 2011.

- [10] H. Lu, S. Liu, H. Wei, and J. Tu, "Multi-kernel fuzzy clustering based on auto-encoder for fmri functional network," *Expert Systems with Applications*, vol. 159, p. 113513, 2020.
- [11] S. Zeng, X. Wang, X. Duan, S. Zeng, Z. Xiao, and D. Feng, "Kernelized mahalanobis distance for fuzzy clustering," *IEEE Transactions on Fuzzy Systems*, vol. 29, no. 10, pp. 3103–3117, 2020.
- [12] W. Xia, Q. Gao, Q. Wang, X. Gao, C. Ding, and D. Tao, "Tensorized bipartite graph learning for multi-view clustering," *IEEE Transactions on Pattern Analysis and Machine Intelligence*, vol. 45, no. 4, pp. 5187–5202, 2022.
- [13] W. Xia, T. Wang, Q. Gao, M. Yang, and X. Gao, "Graph embedding contrastive multi-modal representation learning for clustering," *IEEE Transactions on Image Processing*, vol. 32, pp. 1170–1183, 2023.
- [14] H. Yang, Q. Gao, W. Xia, M. Yang, and X. Gao, "Multiview spectral clustering with bipartite graph," *IEEE Transactions on Image Processing*, vol. 31, pp. 3591–3605, 2022.
- [15] H. Zhao, X. Yang, Z. Wang, E. Yang, and C. Deng, "Graph debiased contrastive learning with joint representation clustering," in *Proceedings of the Thirtieth International Joint Conference on Artificial Intelligence, IJCAI-21*, 2021, pp. 3434–3440.
- [16] J. MacQueen *et al.*, "Some methods for classification and analysis of multivariate observations," in *Proceedings of the fifth Berkeley symposium on mathematical statistics and probability*, vol. 1, no. 14, 1967, pp. 281–297.
- [17] A. Ng, M. Jordan, and Y. Weiss, "On spectral clustering: Analysis and an algorithm," *Advances in neural information processing systems*, vol. 14, 2001.
- [18] U. Von Luxburg, "A tutorial on spectral clustering," *Statistics and computing*, vol. 17, pp. 395–416, 2007.
- [19] F. Nie, X. Wang, and H. Huang, "Clustering and projected clustering with adaptive neighbors," in *Proceedings of the 20th ACM SIGKDD international conference on Knowledge discovery and data mining*, 2014, pp. 977–986.
- [20] J. Han, K. Xiong, and F. Nie, "Orthogonal and nonnegative graph reconstruction for large scale clustering," in *Proceedings of the Twenty-Sixth International Joint Conference on Artificial Intelligence, IJCAI-17*, 2017, pp. 1809–1815.
- [21] S. Pei, F. Nie, R. Wang, and X. Li, "Efficient clustering based on a unified view of k -means and ratio-cut," *Advances in Neural Information Processing Systems*, vol. 33, pp. 14 855–14 866, 2020.
- [22] F. Nie, J. Xue, W. Yu, and X. Li, "Fast clustering with anchor guidance," *IEEE Transactions on Pattern Analysis and Machine Intelligence*, 2023.
- [23] X. He and P. Niyogi, "Locality preserving projections," *Advances in neural information processing systems*, vol. 16, 2003.
- [24] J. Zhou, W. Pedrycz, X. Yue, C. Gao, Z. Lai, and J. Wan, "Projected fuzzy c-means clustering with locality preservation," *Pattern Recognition*, vol. 113, p. 107748, 2021.
- [25] J. Wang, S. Guo, F. Nie, and X. Li, "Local-global fuzzy clustering with anchor graph," *IEEE Transactions on Fuzzy Systems*, vol. 32, no. 1, pp. 188–202, 2024.
- [26] F. Nie, C. Liu, R. Wang, Z. Wang, and X. Li, "Fast fuzzy clustering based on anchor graph," *IEEE Transactions on Fuzzy Systems*, vol. 30, no. 7, pp. 2375–2387, 2022.
- [27] J. Wang, Z. Yang, X. Liu, B. Li, J. Yi, and F. Nie, "Projected fuzzy c-means with probabilistic neighbors," *Information Sciences*, vol. 607, pp. 553–571, 2022.
- [28] X. Zhao, F. Nie, R. Wang, and X. Li, "Robust fuzzy k-means clustering with shrunk patterns learning," *IEEE Transactions on Knowledge and Data Engineering*, 2021.
- [29] G. J. McLachlan, S. X. Lee, and S. I. Rathnayake, "Finite mixture models," *Annual review of statistics and its application*, vol. 6, pp. 355–378, 2019.
- [30] D. A. Reynolds *et al.*, "Gaussian mixture models." *Encyclopedia of biometrics*, vol. 741, no. 659-663, 2009.
- [31] J. Liu, D. Cai, and X. He, "Gaussian mixture model with local consistency," in *Proceedings of the Twenty-Fourth AAAI Conference on Artificial Intelligence AAAI-10*, 2010.
- [32] X. He, D. Cai, Y. Shao, H. Bao, and J. Han, "Laplacian regularized gaussian mixture model for data clustering," *IEEE Transactions on Knowledge and Data Engineering*, vol. 23, no. 9, pp. 1406–1418, 2011.
- [33] F. Pascal, L. Bombrun, J.-Y. Tournier, and Y. Berthoumiou, "Parameter estimation for multivariate generalized gaussian distributions," *IEEE Transactions on Signal Processing*, vol. 61, no. 23, pp. 5960–5971, 2013.
- [34] M. Ahsanullah, B. G. Kibria, and M. Shakil, *Normal and student's t distributions and their applications*. Springer, 2014, vol. 4.
- [35] J. Zhang and F. Liang, "Robust clustering using exponential power mixtures," *Biometrics*, vol. 66, no. 4, pp. 1078–1086, 2010.
- [36] U. J. Dang, R. P. Browne, and P. D. McNicholas, "Mixtures of multivariate power exponential distributions," *Biometrics*, vol. 71, no. 4, pp. 1081–1089, 2015.
- [37] S. Kotz, "Multivariate distributions at a cross road," in *A Modern Course on Statistical Distributions in Scientific Work*. Springer, 1975, pp. 247–270.
- [38] K.-T. Fang, S. Kotz, and K. W. Ng, *Symmetric multivariate and related distributions*. Chapman and Hall/CRC, 2018.
- [39] S. Nadarajah, "The kotz-type distribution with applications," *Statistics: A Journal of Theoretical and Applied Statistics*, vol. 37, no. 4, pp. 341–358, 2003.
- [40] J. A. Bilmes *et al.*, "A gentle tutorial of the em algorithm and its application to parameter estimation for gaussian mixture and hidden markov models," *International computer science institute*, vol. 4, no. 510, p. 126, 1998.
- [41] W. Liu, J. He, and S.-F. Chang, "Large graph construction for scalable semi-supervised learning," in *Proceedings of the 27th international conference on machine learning (ICML-10)*, 2010, pp. 679–686.
- [42] S. P. Boyd and L. Vandenberghe, *Convex optimization*. Cambridge university press, 2004.
- [43] R. A. Horn and C. R. Johnson, *Matrix analysis*. Cambridge university press, 2012.
- [44] F. Nie, J. Xue, D. Wu, R. Wang, H. Li, and X. Li, "Coordinate descent method for k -means," *IEEE Transactions on Pattern Analysis and Machine Intelligence*, vol. 44, no. 5, pp. 2371–2385, 2022.
- [45] A. Fahad, N. Alshatri, Z. Tari, A. Alamri, I. Khalil, A. Y. Zomaya, S. Fofou, and A. Bouras, "A survey of clustering algorithms for big data: Taxonomy and empirical analysis," *IEEE Transactions on Emerging Topics in Computing*, vol. 2, no. 3, pp. 267–279, 2014.